IMPACT OF THE NUMBER OF MRÓZ SURFACES ON THE REPRESENTATION OF THE BAUSCHINGER EFFECT.

Manuscript Info

Manuscript History

Key words:-

Bauschinger Effect, Mróz model, Multisurfaces.

Abstract

This research work analyses the influence of the number of surfaces in the Mróz model on the representation of the Bauschinger effect for two steels (SS-304 and C35). To implement it, we carried out numerical simulations, using a modified Aleksander Karolczuk algorithm, which enabled us to generate stress-strain curves and also to calculate the Bauschinger parameters. The results show that an increased number of surfaces improves accuracy, visible in smoother transitions during loading reversals and stabilisation of parameters. However, an optimal number of surfaces, depending on the material and parameter studied, is required to balance accuracy and computational cost. C35 steel converges faster than SS-304, suggesting less complex behaviour. We have identified a convergence threshold, beyond which increasing the number of surfaces no longer brings significant gains.

Copy Right, IJAR, 2019,. All rights reserved.

1 2

3

5

11

12

13

14

4

1. Introduction

- 6 The plastic modulus function described using piecewise linear representation in multi-surface models. Inevitably,
- 7 the number of surfaces used in this model has an influence on the description and representation of the stress-strain
- 8 relationships for any loading.
- 9 Several questions are addressed concerning the role of the number of surfaces in Mróz's model; it emerges, for example, that:
 - 1. Increasing the number of surfaces improves the accuracy of the plastic modulus function, but at the same time changes the translational behaviour of the surfaces.
 - 2. The advantage of multi-surface models is their ability to reproduce the Bauschinger effect more accurately.
 - 3. This model shows a stress-strain loop that is stabilised from the first cycle any load.
- 15 In particular the second observation will hold our attention in this work: how the number surfaces in Mróz's model
- 16 influences the representation of the Bauschinger effect.
- 17 To conduct this work, we present a general overview of the theory on Bauschinger effect and on the Mróz model.
- 18 Subsequently the methodology of our comparative approach and further on the results obtained.

2. MATERIAL

2.1. Test Material Data

21 The material data used in this work is that of a stainless steel (SS – 304) and that of a calibrated steel (C35) given in

22 table 1 below [1].

Table 1: Material data for SS - 304 stainless sleetand C C35 calibrated

Paramètres		E (MPa)	σ_y (MPa)	σ_L (MPa)	ν	K' (MPa)	n'	G (MPa)
SS-304	Valarina	186 138	241.29	689.4	0.3	1654.56	0.287	71 591
C35	Valeurs	210 00	280	580	0.3	960	0.15	80 000

24

25

19

20

23

2.2. Bauschinger Effect

2627

2930

31

32

33

3435

2.2.1. Definition

In the 1880s, J. Bauschinger [2] [3] proposed four results to express the Bauschinger effect:

- Plastic pre-strain increases yield strength in the same direction as pre-strain;
- Plastic pre-strain reduces the yield strength in the opposite direction to the pre-strain; it may even be reduced to zero;
 - The time between the pre-strain and the reverse strain test has no influence on the new yield strength;
 - Deformation in the opposite direction reduces the elastic limit, and successive deformations in alternating directions lead to a re-increase in this reduced elastic limit, which nevertheless never exceeds its original value.
- 36 Several studies have demonstrated the limitations of this definition by J. Bauschinger. These include works by
- Cottrell [5], Dieter B. [6], Woolley [7], Bueren [8], McClintock [9], Pederson [10], Orowan [11] and Sowerby [12].
- 38 They have shown that the Bauschinger Effect is not limited this simple variation yield strength, but is much more
- 39 complex. As a result, the synthesis of their different approaches to the Bauschinger effect enabled it to be defined as
- the existence on of preformed metals by the difference between the curve (σ, ε) obtained a first loading in one
- 41 direction and that obtained from a loading in the opposite direction (hereinafter referred to as the "second
- direction and that obtained from a loading in the opposite direction (hereinafter referred to as the "second loading").[4].
- 42 loading).[4]
- We will define the variables and concepts that we will use to define the Bauschinger parameters. The main
- quantities involved are defined in Figure 1 below [4]. They are :
- 45 σ_{maxi} : maximum stress reached during the first loading (which is also the strength of the second loading if it carried out in the same direction as the first);
- 47 R_{e_1} : yiel strength of the first load (algebraic value);
- 48 R_{e_2} : yiel strength of the second load (algebraic value);
- 49 ε_{maxi} : maximum total deformation reached during the first loading;
- 50 $ε_{pmaxi}$: maximum plastic strain reached during the first loading;
- 51 β: « Bauschinger deformation » defined at $\sigma = \sigma_{maxi}$;
- 52 $β_n$: « Bauschinger deformation » defined at $σ = n. σ_{maxi}$;

- 53 E_s : difference plastic deformation energy (to reach σ_{maxi} during the second loading), between the material 54 with no Bauschinger effect and the tested material;
 - E_p : plastic deformation energy stored during pre-strain.

57

58

60

55

2.2.2. Characteristic parameters of Bauschinger effect

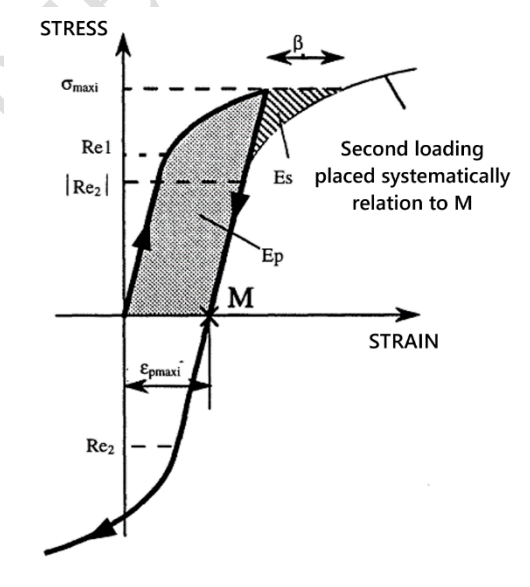
- There are three main categories of parameters used to characterise the Bauschinger effect: stress parameters, strain
- parameters and energy parameters.

Stress parameter

- Bauschinger takes the approach of parameterising this phenomenon in terms of stress; more precisely, it is a ratio of
- elastic limits, or a difference in elastic limits brought back to a reference stress (to obtain a dimensionless quantity).
- 63 Studies show that there are several stress parameters, generally known as the 'Bauschinger stress parameter', which
- can depend on σ_{maxi} : the maximum stress reached during the first loading; the R_{e_1} : the yield strength of the first
- loading and/or the R_{e_2} : the yield strength of the second loading. However, the most commonly used parameter is
- that of AA. Abel et H. Muir [13], which depends on σ_{maxi} and the R_{e_2} , and is expressed as β_{σ} :

$$\beta_{\sigma} = \frac{\sigma_{maxi} + R_{e_2}}{\sigma_{maxi}} = 1 + \frac{R_{e_2}}{\sigma_{maxi}} (1)$$

- When plastic flow in the opposite direction occurs during unloading t (σ >0), R_{e_2} >0, then β_{σ} >1,
- with a theoretical maximum value of 2, i.e. maximum Bauschinger effect.
- When plastic flow starts when the load is reversed (σ <0), R_{e_2} <0 then β_{σ} <1 with a minimum
- theoretical value of 0, i.e. no Bauschinger effect. The Bauschinger effect is illustrated in Figure 1
- 71 below [4].



72 73

Figure 1: Bauschinger effect presentation

Strain parameters

75

76 77

78

79

80

82

Figure 2 below graphically illustrates all the parameters of the Baushinger effect. In the deformation parameter approach, J. Bauschinger considers that the Bauschinger deformation parameter describes the amplitude of deformation in the opposite direction required to achieve the level of prestress. More or less satisfactory research work has produced various expressions of this approach; for the following, we will use Abel's approach, which is better suited to low-cycle fatigue.

The «Bauschinger strain parameter », β_{ε} proposed by Abel, is defined as the ratio of the « Bauschinger

deformation», définiedby Woolley (with n=1) on the plastic predeformation, ε_{pmaxi} :

$$\beta_{\varepsilon} = \frac{\varepsilon_r}{\varepsilon_{pmaxi}} \quad (2)$$

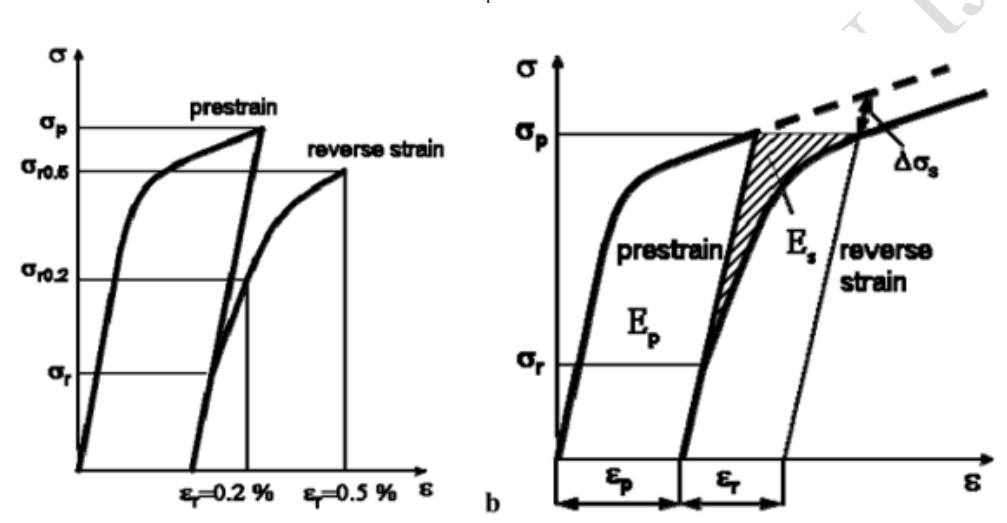


Figure 2: Representation of Bauschinger effect parameters

85

83

84

86

89 90

92

94

95

Energy parameters

The Bauschinger energy parameter describes amount of energy required during reverse deformation to reach the stress level of the first loading.

Abel, then, defines β_E as the energy « recovered » during the second loading E_S , compared with the energy « stored » during the first loading, E_P :

$$\beta_E = \frac{E_S}{E_B} \quad (3)$$

 E_S is the energy «recovered» during reverse loading, up to the same maximum stress on initial loading;

 E_p is the plastic deformation energy dissipated during the first loading, to reach the total pre-strain ε_{maxi} .

In absence of the Bauschinger effect, E_S is null, as is β_E .

In the presence of the Bauschinger effect, E_S represents the energy that does not need to supplied during the second load, because it was « reversibly» stored during the first load.

 E_S , defined by Abel « Bauschinger energy », represents the difference in energy required to reach σ_{maxi} during the second loading, between a material without Bauschinger effect and the tested material.

98

99

96 97

Average Bauschinger strain parameter: A.B.S (Average Bauschinger Strain)

This parameter, proposed by Saleh and Margolin [SAL79] to study the Bauschinger effect on certain alloys, is used to account for the fact that the Bauschinger strain is a continuously variable quantity, from the start of the reverse plastic flow, until complete stress inversion. Its expression is given by:

$$A.B.S. = \frac{E_S}{\sigma_{maxi}}$$
 (4)

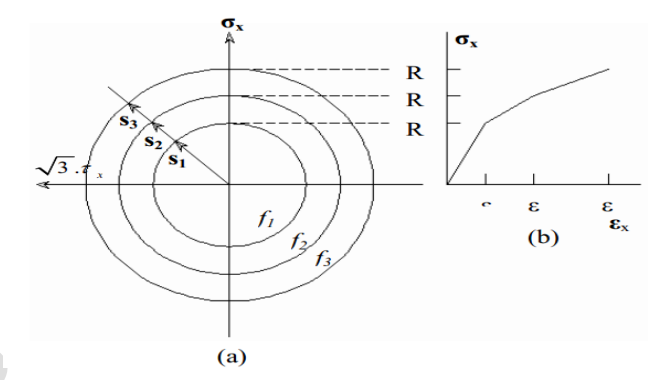
103

104

2.3. Multisurfaces model of Mróz

The Mróz model [14], also known as Multilayer or Multisurface, is a three-dimensional generalisation of the Saint-Venant model.

For a better approximation of the stress-strain curve and a generalisation of the plastic modulus in the multiaxial model, Mróz defined a field of different plastic moduli in stress space; he introduced several charge surfaces each with a radius and a centre (Figure 3).



110111

Figure 3 : MROZ model

The multi-layer mathematical model of Mróz is characterised by the expressions below:

114
$$\underline{\boldsymbol{\varepsilon}}^t = \underline{\boldsymbol{\varepsilon}}^e + \underline{\boldsymbol{\varepsilon}}^p$$
 (5)(Total deformation)

115
$$f_i = J_2(\underline{\sigma} - \underline{X}^i) - R^i$$
 (6) (Load function)

116
$$\dot{\mathcal{E}}^p = n^a \dot{\lambda}^a = \frac{1}{C^a} \frac{\langle \underline{n}_{\underline{a}}^a : \dot{\underline{a}}_{\underline{a}} \rangle}{\underline{n}^a : \underline{n}^a} \frac{\partial f^a}{\partial \underline{\sigma}}$$
 (7) (Evolution of plastic deformation)

117
$$\mathbf{\dot{X}}^{a} = \Delta_{a}^{a+1} \dot{\boldsymbol{\mu}}$$
 (8) (Evolution of internal stresses)

118
$$\Delta_{\underline{a}}^{a+1} = \frac{\left[(R^{a+1} - R^a) \underline{\sigma} - (R^{a+1} \underline{X}_{\underline{a}}^a - R^a \underline{X}_{\underline{a}}^{a+1}) \right]}{R^a}$$
 (9) (Direction vector)

119
$$\dot{\boldsymbol{\mu}} = \frac{\langle \underline{\underline{n}}^{\underline{a}} : \dot{\underline{\sigma}} \rangle}{\underline{n}^{\underline{a}} : \underline{\Delta}^{\underline{a}+1}}$$
 (10) (flow intensity)

121 3. METHODOLOGY

The methodology we used to analyze the impact of the number of Mróz surfaces on the representation of the Bauschinger effect is based on an approach combining numerical simulation and graphical analysis, applied to two steel grades (SS-304 and C35). A modified Aleksander Karolczuk algorithm was used to simulate Mróz's model. For each number of surfaces considered (2, 3, 5, 9, 17, 33), we ran a simulation, obtaining the stress-strain hysteresis curve. The hysteresis curves we simulated were then plotted to visualize the Bauschinger effect and its evolution as a function of the number of surfaces. A graphical analysis the symmetry with respect to point M (Figure 1) enabled us to represent Bauschinger energy profile. We then calculated the Bauschinger parameters (β_{σ} , β_{ε} , A.B.S, β_{ε}) for each number of surfaces using the formulae presented in Table 2. These parameters allowed us to quantify the Bauschinger effect and its evolution. Next, we evaluated the Bauschinger parameters and the hysteresis curves were analyzed graphically and numerically to determine the number of surfaces required for the model to converge. Subsequently we also analyzed the influence of the size of the plastic domain ($\Delta \sigma$) on the number of surfaces required for convergence. Finally, we compared the results for the two steels (SS-304 and C35), highlighting the influence of material properties on the optimum number of surfaces and the representation of the Bauschinger effect. Appendix 1 presents a summary of our methodological approach in the form of a simplified diagram.

4. RESULTATS AND DISCUSSIONS

In Mróz's work, research [14], [15] demonstrates that increasing the number of surfaces improves the accuracy of the plastic modulus function while modifying the surface translation behaviour. These works also point out that multisurface models have the advantage of reproducing the Bauschinger effect more accurately. Our work in this paper provides a graphical illustration of this observation. In this work, we present variants of the representation of the Bauschinger effect as a function of the number of surfaces in a uni-axial load approach for tests carried out on a SS- stainless steel and a C35 graded steel.

4.1. Analyses of the influence of the number of Mróz surface on the representation of the Bauschinger effect (SS

146 - **304**)

4.1.1. Assessment of Bauschinger parameters

- Several researchers [13], [16], [17], [18] have proposed expressions or formulae for calculating Bauschinger parameters. Figure 4 below is a graphical representation of the Bauschinger effect for SS 304 stainless steel. After plastic deformation in tension (up to σ_{max}), the compressive yield strength (R_{e2}) is lower than the initial tensile yield strength. This is the manifestation of the Bauschinger effect. Figure 5 below illustrates the A graphical representation of the variables used to estimate the Bauschinger parameters, it breaks down the cyclic curve to illustrate the parameters used to quantify the Bauschinger effect:
- ε_p : Plastic deformation during initial loading.
- ε_r : Inverse deformation (in this case in compression) required to reach the elastic limit in compression.
- E_n : Plastic deformation energy initial loading.
- E_s : Deformation energy during unloading and reverse reloading up to the elastic limit.

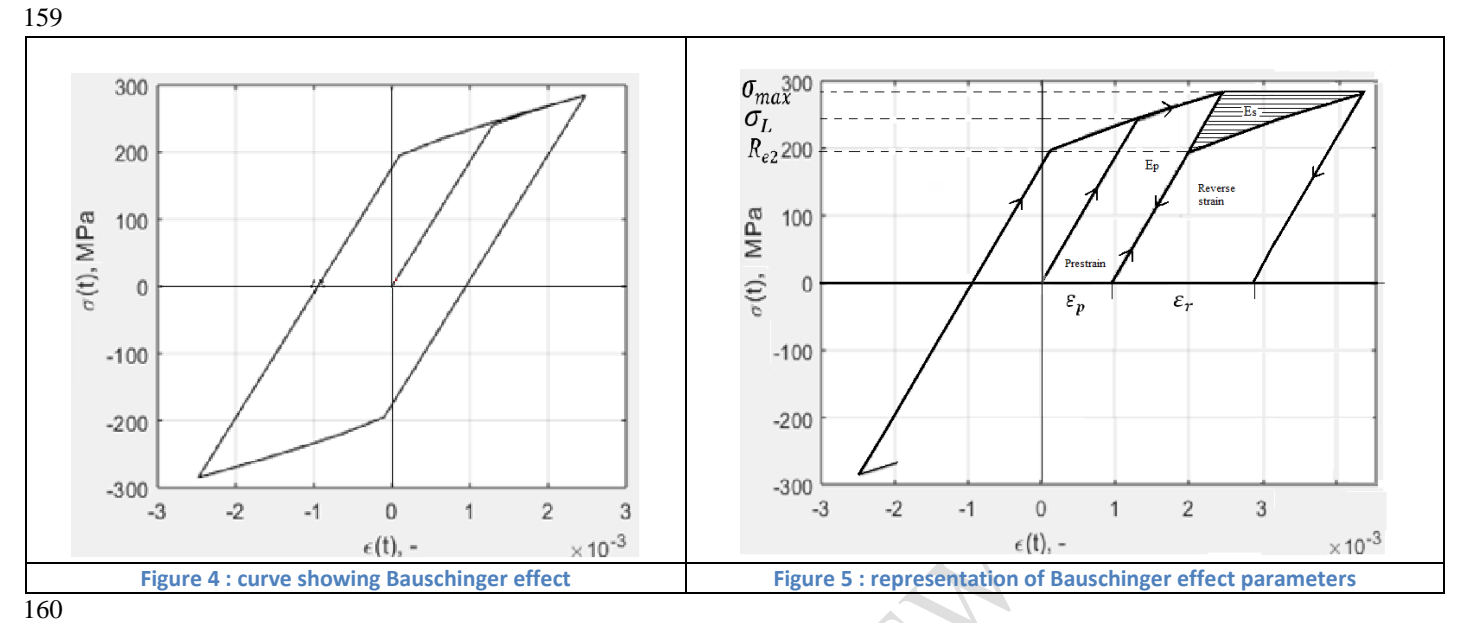


Table 2 below defines the Bauschinger parameters used to quantify the effect. These parameters are ratios or differences between the values measured on the cyclic curve as shown in Figure 5.

Table 3 illustrates the process of numerically calculating the parameters for SS-304 stainless steel.

Tableau 2: Expression of Bauschinger parameters

Bauschinger parameter	Expression
Stress parameter (β_{σ})	$\beta_{\sigma} = 1 - \left(\frac{R_{e2}}{\sigma_{max}}\right)$
Deformation parameter (β_{ε})	$eta_arepsilon = rac{arepsilon_r}{arepsilon_p}$
ABS parameter (Average Bauschinger Strain)	$A.B.S = \frac{E_s}{\sigma_{max}}$
Energy parameter (β_E)	$eta_E = rac{E_s}{E_p}$

Tableau 3 : Calcul of Bauschinger parameters

Value of input variables for calculating Bauschinger parameters								chinger	parameter	s values
σ_{max} (MPa)	σ_L (MPa)	R_{e2} (MPa)	$arepsilon_p$	ε_r	$E_{\scriptscriptstyle S}$	E_p	eta_{σ}	$eta_{arepsilon}$	A. B. S	eta_E
290	241.29	191.25	0.1%	0.2%	389.92	1122.31	0.34	2	1.34	0.35

4.1.2. Analyses of influence of the number of surfaces

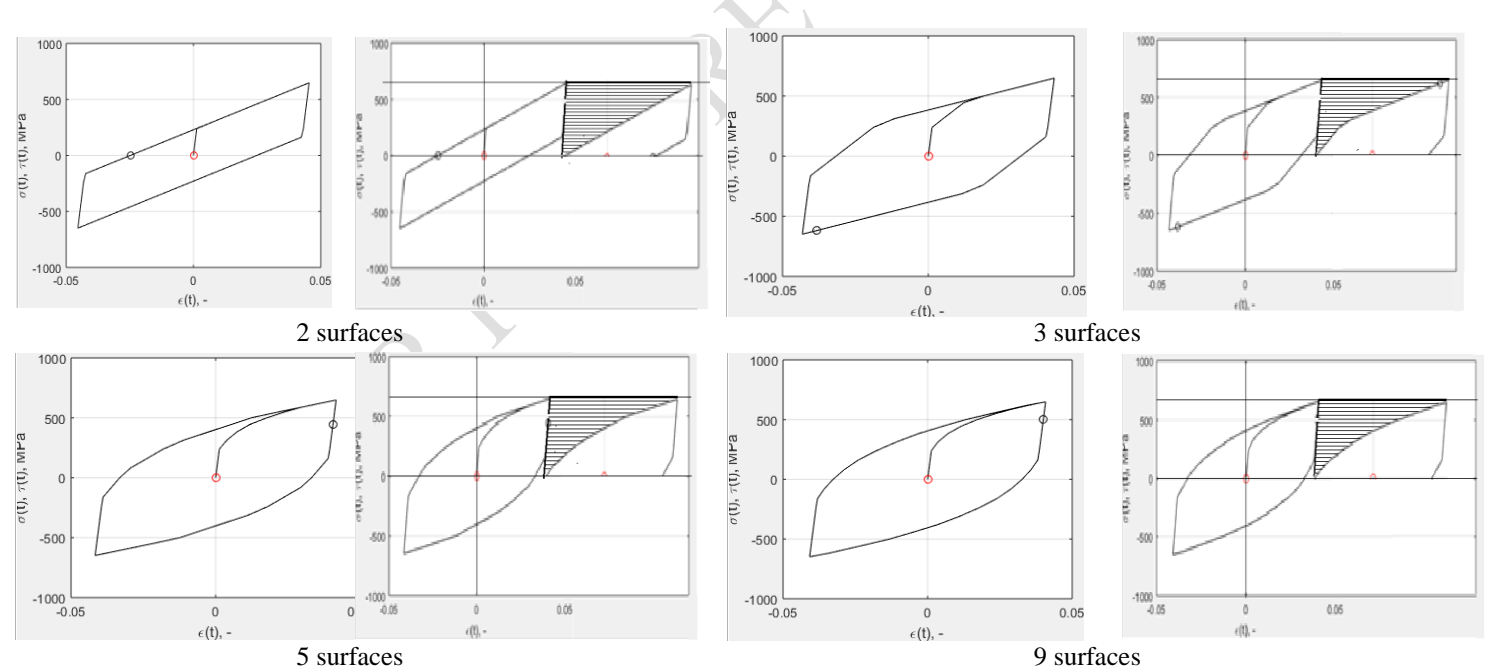
4.1.2.1. Influence on the representation of the Bauschinger effect

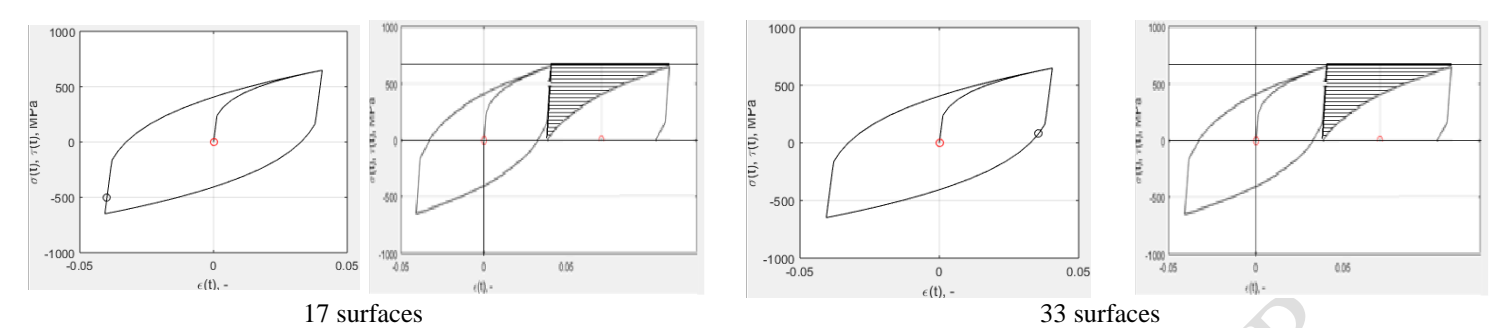
The figures presented in Table 4 below clearly show the influence of the number of surfaces in a Mróz-type model on the representation of the Bauschinger effect. We can see that as the number of surfaces increases, the simulated stress-strain curve approaches a smooth behaviour when the loading is reversed.

We note with a small number of surfaces (2, 3 and 5), the transition between loading and unloading is abrupt, creating corners on the curve. This represents a rough approximation of the Bauschinger effect. The model has difficulty in capturing the gradual transition between tensile and compressive behaviour. Then, by increasing the number of surfaces (9 and 17), the transition is smoothed out and the curvature observed experimentally when the loading is reversed is better represented. The Bauschinger effect is better reproduced. And with a large number of surfaces (33), the curve becomes very smooth and approaches continuous behaviour. The transition between tension and compression is almost imperceptible, which corresponds to a more realistic representation of the Bauschinger effect in this material. These figures therefore directly illustrate the part of the assertion concerning the improvement in accuracy with an increase in the number of surfaces; the more surfaces there are, the more accurately the model can reproduce the changes in slope during load reversals, which is characteristic of the Bauschinger effect.

We can see that the improvement in the accuracy of the plastic modulus is reflected in the model's ability to reproduce changes in the slope of the stress-strain curve. A model with few surfaces will have abrupt changes in tangent modulus, whereas a model with many surfaces will have a smoother and continuous variation of the tangent modulus, closer to reality. We also point out that although the translational behaviour of the surfaces is not directly visible in these figures, the evolution the Bauschinger effect over repeated loading cycles is linked to the translation of the loading surfaces in the stress space. It is this translation mechanism that allows Mróz's model to capture the loading history and its influence on the material's behaviour.

Tableau 4: Evolution of the representation of the Bauschinger effect as a function of the number of surfaces - SS - 304





4.1.2.2. Influence on Bauschinger parameters

The evolution of the values of the Bauschinger parameters as a function of the number of surface areas obtained is shown in Table 5 below and the graphical representation of this evolution is shown in Table 6 below. Analysis of the graphs representing the parameters shows that:

- Stress Indicator (β_{σ}): this parameter remains constant at 1, regardless of the number of surfaces. This is because R_{e2} (compressive yield strength) is equal to 0 in all cases presented. Therefore, $\beta_{\sigma} = 1 \left(\frac{R_{e2}}{\sigma_{max}}\right) = 1 \left(\frac{0}{645}\right) = 1$.
- **Energy Indicator** (β_E) :the energy indicator stabilises from approximately 9 surfaces. This suggests that beyond a certain number of surfaces, the energy dissipated during inversions is correctly captured by the model.
- **Strain Indicator** (β_{ε}): this parameter also stabilises at around 9 surfaces. This indicates that the deformation required to reach the strain parameter is well represented with a sufficient number of surfaces.
- A.B.S Indicator: similar to the other indicators, the A.B.S stabilises after a few surfaces.

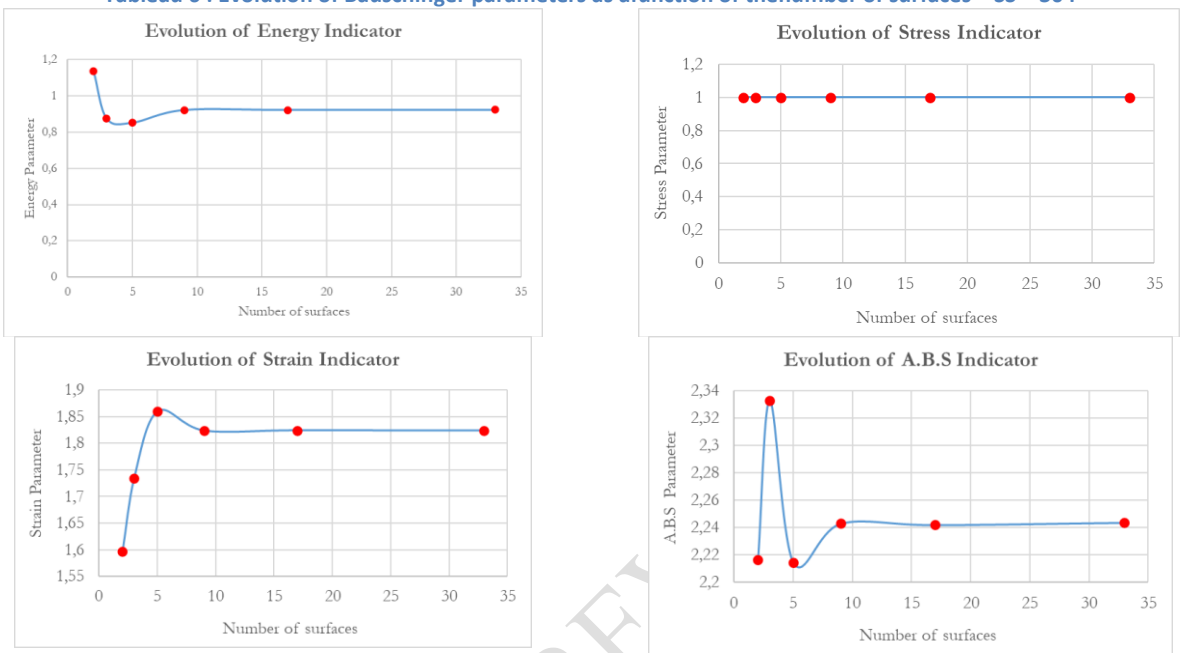
Overall, these graphs show that the Bauschinger parameters stabilise as the number of surfaces increases. This indirectly suggests an improvement in the accuracy of the tangent plastic modulus, since a better representation of the Bauschinger effect implies a better capture of variations in the slope of the stress-strain curve. Note that the stabilisation of the Bauschinger parameters may be a consequence of the way the surfaces translate and interact in the Mróz model, so increasing the number of surfaces allows greater flexibility in describing surface translations and gives a better representation of the Bauschinger effect. The graphs in Table 6 also clearly show that the multisurface model is capable of reproducing the Bauschinger effect and that the accuracy of this reproduction improves with the number of surfaces, up to a certain point where stabilisation is reached.

Tableau 5: Estimation of Bauschinger effect parameters as a function of the number of surfaces - SS - 304

Number of	Input variables for calculating Bauschinger parameters Bauschinger parameters Bauschinger parameters									eters
surfaces	σ _{max} (MPa)	R_{e2} (MPa)	$arepsilon_p$	ϵ_r	\boldsymbol{E}_{s}	$\boldsymbol{E_p}$	$oldsymbol{eta}_{\sigma}$	$oldsymbol{eta}_{arepsilon}$	A. B. S	$oldsymbol{eta}_E$
2 surfaces	645	0	0.0429	0.0685	1429.68	1258.22	1	1.5967	2.2165	1.1362
3 surfaces	645	0	0.0415	0.0720	1505.23	1720.28	1	1.7345	2.333	0.8750

5 surfaces	645	0	0.0398	0.074	1428.45	1676.08	1	1.8593	2.2146	0.8522
9 surfaces	645	0	0.0385	0.0702	1446.75	1567.99	1	1.8234	2.243	0.9227
17 surfaces	645	0	0.0387	0.0710	1446.13	1566.57	1	1.8239	2.242	0.9231
33 surfaces	645	0	0.0386	0.0709	1447.21	1567.39	1	1.8236	2.2437	0.9233

Tableau 6: Evolution of Bauschinger parameters as afunction of thenumber of surfaces - SS - 304



4.1.2.3. Number of threshold areas

Figure 6 and Table 7 show the relationship between the size of the plastic domain (represented by $\Delta\sigma$ and σ_{max}) and the number of surfaces required for convergence in the Mróz model. In the context of the Mróz model, convergence means that the predictions of the model stabilize and do not change significantly with a further increase in the number of surfaces. This is similar to what we observed in the previous graphs of Bauschinger parameters in Table 6.

 $\Delta\sigma$ represents the difference between the maximum stress (σ_{max}) and the initial yield strength (σ_y). This is a measure of the depth of plastic deformation of the material. σ_{max} also reflects the extent of plastic deformation. Figure 6 and Table 7 show that for smaller plastic domains ($\Delta\sigma$ and σ_{max}), fewer surfaces are required for convergence. As the plastic domain extends (higher $\Delta\sigma$ and σ_{max}), the number of surfaces required for convergence increases, then stabilizes at 9 surfaces.

The results obtained in Table 7 reinforce the idea that a higher number of surfaces leads to greater accuracy, particularly when modelling large plastic deformations. For small plastic deformations, a few surfaces may be sufficient. But as the plastic domain grows, more surfaces are needed to capture the complex evolution of the loading surface and accurately represent the Bauschinger effect. This is because larger plastic deformations imply more complex interactions between the multiple loading surfaces in the Mróz model.

It is important to note that the increasing number of surfaces required to converge for larger plastic domains reflects the greater complexity of the translation and deformation of these surfaces. With larger plastic deformations, the load surfaces undergo more significant translations and distortions, requiring finer discretization (more surfaces) to accurately model this behavior. Figure 6 also highlights the consideration that using an excessively large number of surfaces may not provide significant improvements in accuracy, but will increase the computational cost. Stabilization from the number of surfaces to 9 for larger $\Delta \sigma$ suggests an optimal balance between accuracy and

241 computational efficiency in this particular example.

242 Tableau 7: Evolution du domaine plastique en fonction du nombre de surface

$\Delta \sigma = \sigma_{max} - \sigma_{y} \text{ (MPa)}$	σ_{max} (MPa)	Number of convengence surface
0	241.29	1
55	296.29	5
110	351.29	9
165	406.29	9
220	461.29	9
275	516.29	9
330	571.29	9
385	626.29	9
440	681.29	9

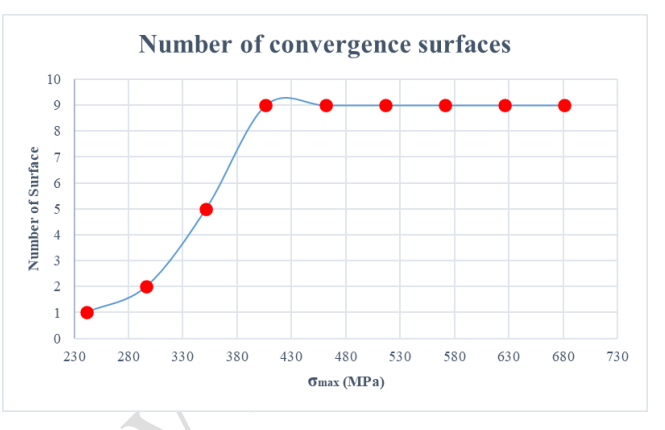


Figure 6: Number of convergence surface

243

244

245

246

247248

249

250

251

252

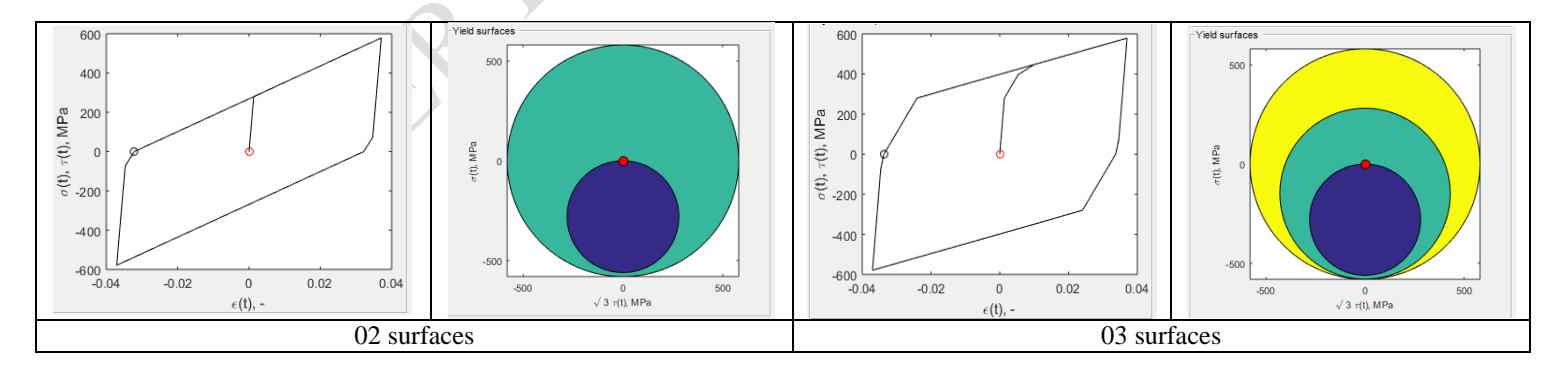
253

4.2. Analysis of influence of the number of Mroz surfaces on the representation of the Bauschinger effect and its parameters (C 35)

Tables 8, 9 and 10 give a similar analysis to that in section 4.1, but this time for a C35 steel. Our analysis still explores the influence of the number of Mróz surfaces on the representation of the Bauschinger effect and the calculation of its parameters.

The figures in Table 8 below show the progression of the loading surface in stress space (represented by the concentric circles) and the stress-strain curve for different numbers of surfaces (2, 5, 9, 17, 33). Once again, we see that increasing the number of surfaces results in a smoother transition when the loading is reversed, refining the representation of the Bauschinger effect.

Tableau 8: Evolution of the representation of Bauschinger effect according to the number of surfaces for a C 35 steel



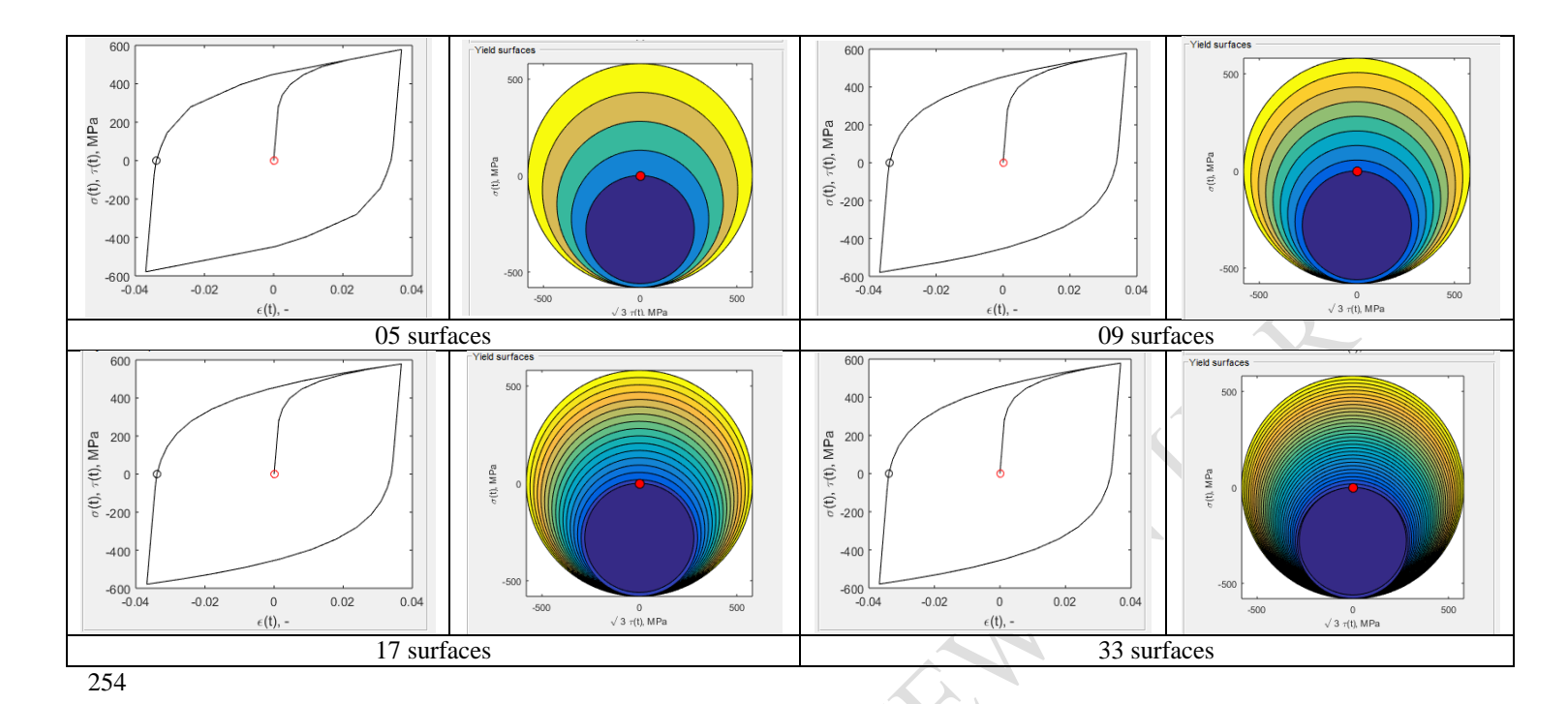


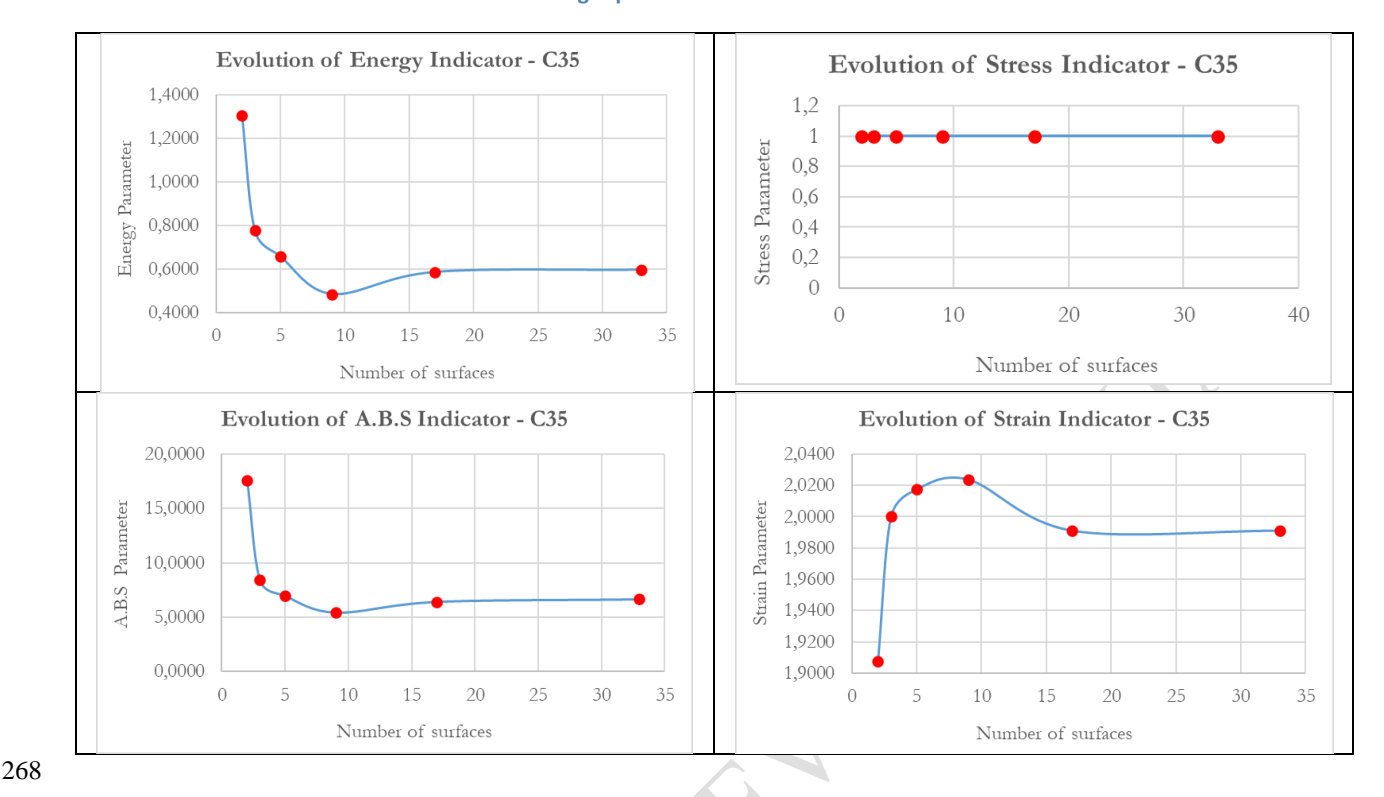
Table 9 below gives the values of the Bauschinger parameters (β_{σ} , β_{ε} , A.B.S, β_{E}) calculated for each number of surfaces. The graphs in Table 10 show the evolution of these parameters as a function of the number of surfaces. We find that the stress indicator β_{σ} also remains constant at one as R_{e2} is zero. The other parameters β_{ε} , A.B.S, and β_{E} evolve with the number of surfaces, then tend to stabilize. We observe a faster convergence for C35 than for SS-304, with a stabilization around 5 to 9 surfaces.

The faster stabilization of the parameters for C35 suggests that the behaviour of this material under load reversals is potentially less complex than that of SS-304, and therefore requires fewer surfaces for accurate representation. This analysis suggests that the optimum number of surfaces depends on the material and its specific behaviour. This means that what is optimal for C35 may not be optimal for another material. These results suggest the importance of calibrating Mróz's model with experimental data to determine the optimal number of surfaces for a given material.

Tableau 9: Estimation of Bauschinger parameters as a function number of surfaces - C- 35

Number of surfaces	Input variables for calculating the Bauschinger parameters							Bauschinger parameters					
	σ _{max} (MPa)	R_{e2} (MPa)	$\varepsilon_p\%$	$\varepsilon_r\%$	\boldsymbol{E}_{s}	E_p	$\boldsymbol{\beta}_{\sigma}$	$oldsymbol{eta}_{arepsilon}$	A. B. S	β_E			
2 surfaces	568	0	3.47	6.62	9984.62	7657.04	1	1.9078	17.5786	1.3040			
3 surfaces	568	0	3.35	6.7	4808.75	6196.94	1	2.0000	8.4661	0.7760			
5 surfaces	568	0	3.39	6.84	3956.70	6022.29	1	2.0177	6.9660	0.6570			
9 surfaces	568	0	3.35	6.78	3081.57	6360.49	1	2.0239	5.4253	0.4845			
17 surfaces	568	0	3.42	6.81	3644.12	6217.82	1	1.9912	6.4157	0.5861			
33 surfaces	568	0	3.42	6.81	3779.24	6338.09	1	1.9912	6.6536	0.5963			

Tableau 10: Evolution of Bauschinger parameters as a function of the number of surfaces - C 35



4.3. Comparison of Bauschinger parameters SS - 304 stainless with those for C 35 calibrated steel

In this section we compare the Bauschinger effect parameters for SS - 304 and C 35 steels, and highlight the number of surfaces required for convergence in each case. A priori we observe that the stability of the Bauschinger parameters indicates convergence in both cases: for SS - 304, convergence is achieved with fewer surfaces for the strain and energy indicators (9 surfaces) compared to the A.B.S parameter (17 surfaces); and for C35, convergence is achieved from 17 surfaces for these three parameters (β_{ε} , A.B.S, et β_{E}).

The different convergence behaviour of these two steels allows us to observe the importance of material properties in determining the optimum number of surfaces for the Mróz model. We found that SS - 304 requires fewer surfaces for certain parameters (β_{ε} , and β_{ε}), which shows potentially less complex behaviour in the case of reverse loading compared with C35. The fact that the A.B.S indicator requires more surfaces for convergence in SS-304, indicates that this parameter is more sensitive to the number of surfaces and may represent a more nuanced aspect of the Bauschinger effect in this material. The general trend of convergence of the Bauschinger parameters with increasing number of surfaces allows us to support the initial argument that a higher number of surfaces generally improves the accuracy of the Mróz model in representing the Bauschinger effect.

Overall, this comparison highlights the need for careful calibration of the Mróz model. In this context, we deduce from our research that the optimal number of surfaces is not universal and must be determined according to the specific material being modelled and the desired level of accuracy for each Bauschinger parameter. So ultimately, using too few surfaces can lead to inaccurate predictions, while using too many surfaces increases the computational cost without significant gains in accuracy.

5. CONCLUSION

- Our research initially explored the influence of the number of surfaces in the Mróz model on the representation of
- 291 the Bauschinger effect, a crucial phenomenon in plasticity. And the study, combining numerical simulations and
- graphical analyses, using a modified Aleksander Karolczuk algorithm applied to two grades of steel: SS-304 and
- 293 C35.

289

- 294 The results we obtained confirm that increasing the number of surfaces improves the accuracy of the representation
- of the Bauschinger effect. We found that the simulated stress-strain curves show smoother transitions during loading
- reversals as the number of surfaces increases. This smoothing means that we can observe a better capture of the
- 297 material's actual behaviour, particularly in terms of the tangent modulus. In quantitative terms, this improvement is
- reflected in the stabilisation of the Bauschinger parameters (β_{σ} , β_{F} , A.B.S, β_{F}) calculated for each simulation.
- 299 Our research highlights the importance of model calibration. We have found that the optimum number of surfaces is
- 300 not universal: it varies according to the material and even depends on the Bauschinger parameter considered. For
- example, C35 converges more quickly than SS-304, suggesting less complex load reversal behaviour. For SS-304,
- 302 the A.B.S. indicator requires more surfaces to converge, highlighting its sensitivity to the discretisation of the model.
- The analysis of the size of the plastic domain ($\Delta \sigma$) revealed to us the existence of a threshold beyond which
- increasing the number of surfaces no longer significantly improves the accuracy, but unnecessarily increases the
- 305 computational cost. This threshold, which we observed at around 9 surfaces for the SS-304, allows us to optimise
- 306 the model by striking a balance between accuracy and efficiency. Thus, by using the mainly graphical approach to
- 307 determine this threshold, our work has also enabled us to confirm the value of Mróz'smultisurface models for
- 308 representing the Bauschinger effect. Future work could explore a more in-depth theoretical justification to refine the
- determination of the optimal number of surfaces and consolidate the conclusions of this study.

311 REFERENCES

- Christine CROS, « Etude d'un modèle incrémental de plasticité cyclique pour une méthode de prédiction de
- [1] durée de vie en fatigue multiaxiale aléatoire », Mémoire DEA Juillet 1994 ; ECL, Université Claude Bernard-Lyon I.
 - J. Bauschinger, « Ueber die Verdnderung der Elasticitdtsgrenze und des Elasticitdtsmodulusverschiedener
- [2] Me talle (On the changes of the Elastic Limit and Elastic Modulus of Various Metals) », Civiling N.F; Vol. 27 N°19, 1881, pp. 289-348.
 - J. Bauschinger, (1887) « Variations in the elastic limit of iron and steel » (traductionrésumée de «
- [3] MitterlungenausdemMechanischenLaboratorium der K. Hochschule in München»), Journal of The Iron and Steel Institute, Vol.1, pp. 442-444.

 Mélanie CHOTEAU, « CARACTERISATION DE L'EFFET BAUSCHINGER EN SOLLICITATIONS
- [4] UNIAXIALES D'UN ACIER INOXYDABLE AUSTENITIQUE X2CrNiMo17-12-2 », Thèse de Doctorat, 1999, UNIVERSITE DES SCIENCES ET TECHNIQUES DE LILLE FLANDRES-ARTOIS.
- [5] A.H. Cottrell, « *Dislocations and plastic flow in crystals* », Oxford UniversityPress, Oxford, 1953, pp.lll-116
- [6] S.N. Buckley et K.M. Entwistle, « *The Bauschinger effect in super-pure aluminium single crystals and polycrystals* » , acta metallurgica, Vol.4 N°4,1956, pp. 325-361.
- [7] R.L. Woolley, « The Bausch inger effect in sorne face-centred and bodycentredcubic metals», Philosophical Magazine, Vol. 44 N°353, 1953, pp. 597-618.
- [8] H.G. Van Bueren, «Imperfections in crystal», North Bolland Amsterdam, 1960, p. 240.
- [9] F.A. McClintock et A.S. Argon, « *Mechanical Behaviour of Materials*» , Addison-Wesley, MA, 1966, pp. 185.
- [10] O.B. Pederson, L.M. Brown, and W.M. Stobbs, « *The Bauschinger effect in copper* », Acta metallurgica, Vol29, 1981, pp. 1843-1850.
- [11] R. Orowan, «Internai Stress and Fatigue in Metals », Elsevier, New York, 1959, p.59.
- [12] R. Sowerby et D.K. Uko, « A Review of Certains Aspects of the Bausch ingerEffect in Metals », Materials Science and Engineering, Vol. 41, 1979, pp. 43-58.

- [13] A. Abel et H. Muir, «A new look at the Bauschinger effect », MetalsAustralia, Vol. 4N°8, September 1972, pp. 267-271.
- [14] Mróz, Z. (1967). "On the description of anisotropic workhardening." Journal of the Mechanics and Physics of Solids, 15(3), 163-175.
- [15] Mróz, Z. (1969). "An attempt to describe the behavior of metals under cyclic loads using a more general workhardening model." Acta Mechanica, 7, 199-212.
- [16] Tan, X., et al. (2016). "Parameters characterizing the Bauschinger effect in steels." Materials Science and Engineering: A, Vol. 660, 101-107.
- Yoshida, K. and Kuwabara, T. (2007). "Effect of strain hardening behavior on forming limit stresses of steel tube subjected to nonproportional loading paths." International Journal of Plasticity, 23(7), 1260-1284.
- [18] Hu, X., et al. (1992). "New parameters for characterizing the Bauschinger effect." Materials Science and Engineering: A, 145(2), 281-287.

312 I. APPENDICES

313 Appendix 1: Methodological Diagram

